J. Biochem. 2010;147(6):843–850 doi:10.1093/jb/mvq017

JB THE JOURNAL OF BIOCHEMISTRY

The functional organization of the internal components of *Rice dwarf virus*

Received December 3, 2009; accepted February 10, 2010; published online February 26, 2010

Naoyuki Miyazaki[1,2,3,4,*], Bomu Wu[2], Kyoji Hagiwara[3], Che-Yen Wang[1], Li Xing[1], Lena Hammar[2], Akifumi Higashiura[4], Tomitake Tsukihara[4], Atsushi Nakagawa[4], Toshihiro Omura[3] and R. Holland Cheng[1,2,†]

[1]Department of Molecular and Cellular Biology, University of California, Davis, CA 95616, USA; [2]Karolinska Institute Structural Virology, 14157 Huddinge, Sweden; [3]National Agricultural Research Center, 3-1-1 Kannondai, Tsukuba, Ibaraki 305-8666; and [4]Institute for Protein Research, Osaka University, 3-2 Yamadaoka, Suita, Osaka 565-0871, Japan

*Naoyuki Miyazaki, Institute for Protein Research, 3-2 Yamadaoka, Suita, Osaka 565-0871, Japan, Tel.: +81 6 6879 8608, Fax: +81 6 6879 8609, email: naomiyazaki@protein.osaka-u.ac.jp

†R. Holland Cheng, Department of Molecular and Cellular Biology, University of California, Davis, CA 95616, USA, Tel./Fax: +1 530 752 5659, email: rhch@ucdavis.edu

The capsid structures of particles of *Rice dwarf virus* that consisted of different components, namely, intact particles, empty particles lacking the 12 segments of double-stranded RNA (dsRNA), and virus-like particles composed of only the P3 core and P8 outer capsid proteins, generated with a baculovirus gene-expression system, were determined by cryo-electron microscopy. Combining the results with those of biochemical analysis, we assigned proteins of the transcriptional machinery and dsRNA to density clusters around the 5-fold axes and along the radial concentric layers, respectively. P7 protein, a component of the transcriptional machinery, was assigned to the outermost region of the density clusters. The density connecting the transcription complex to the outermost RNA densities implied interactions between the dsRNA and the P7 protein. Our structural analysis and the non-specific nucleic acid-binding activity of P7 explain the spiral organization of dsRNA around the 5-fold axis.

Keywords: electron microscopy/genome organization/*Phytoreovirus*/*Rice dwarf virus*/transcription.

Abbreviations: BTV, *Bluetongue virus*; CPV, *Cytoplasmic polyhedrosis virus*; Cryo-EM, cryo-electron microscopy; dsRNA, double-stranded RNA; eRDV, empty RDV; fRDV, full RDV; RDV, *Rice dwarf virus*; RRSV, *Rice ragged stunt virus*; TC, Transcriptional complex; VLP, Virus-like particle.

Rice dwarf virus (RDV) has an icosahedral double-shelled capsid of approximately 700 Å in diameter. The virus is a member of the genus *Phytoreovirus,* in the family *Reoviridae*, and is transmitted by insect vectors to rice, wheat, barley, and other graminous plants. RDV has seven structural proteins, namely, P1, P2, P3, P5, P7, P8 and P9 (*1*, *2*). The core of RDV consists of 120 copies of asymmetric dimers of P3 protein, which enclose 12 segments of double-stranded RNA (dsRNA); the P1 protein, which is a putative RNA-dependent RNA polymerase; the P5 protein, which is a putative guanylyltransferase; and the P7 protein, which is a non-specific nucleic acid-binding protein (*1*). The core is surrounded by 780 copies of the P8 outer capsid protein, and a double-layered capsid is assembled with disparate icosahedral lattices (*3*, *4*). A small number of P9 (*5*) and P2 (*1*) protein molecules are associated with the capsid and are required for vector-mediated transmission of the virus.

The genomes of viruses in the *Reoviridae* are transcribed inside the intact capsid, and nascent mRNA is capped before it is released from the intact capsid. Reoviruses can be divided; in structural terms, into two subgroups (*6*) with the capsid having either a complete $T = 13l$ layer e.g. RDV (*4*), bluetongue virus (BTV) (*7*) and rotavirus (*8*) or an incomplete $T = 13l$ layer e.g. reovirus (*9*), *Cytoplasmic polyhedrosis virus* (CPV) (*10*), and *Rice ragged stunt virus* (RRSV) (*11*). Unlike the viruses with an incomplete $T = 13l$ capsid with exposure of the capping enzymes outside the inner shell, the complete $T = 13l$ second-layered viruses contain all necessary transcriptional enzymes, with polymerase, helicase, guanylyltransferase and transmethylase activities, within their shell. In the former case, the structural analysis of reovirus has provided a detailed description of the structural and functional organization of the transcriptional enzymes (*12*). However, in the latter case, the transcriptional process must be accomplished by all four enzymatic activities before the product is exported through the innermost capsid shell. Thus, the arrangement of the transcriptional enzymes of complete $T = 13l$ type viruses seems likely to be different from that of viruses of the incomplete $T = 13l$ type. The internal proteins of complete $T = 13l$ second-layered viruses are generally believed to form an RNA-binding cluster, known as a transcriptional complex (TC), to ensure appropriate completion of transcription. In the case of RDV, biochemical analysis suggests that each TC consists of one copy each of the P1 and P5 proteins and five copies of the P7 protein. However, the organization of the TC and details of the mechanism of transcription remains to be clarified.

The structure of the RDV particle has been determined at 3.5 Å resolution by X-ray crystallography (*4*). However, at lower resolution, the electron density map showed a few layers of RNA density inside the capsid

layer and a density mass at each 5-fold vertex, but this density gradually disappeared with increasing resolution during phase extension and it was disordered at 3.5 Å resolution. Thus, the resulting atomic model consisted of P3 and P8 capsid proteins and fragments of P7 protein. These observations indicated that neither the dsRNA segments nor the transcriptional enzymes inside the capsid shell are spatially ordered at near-atomic resolution. Therefore, the internal structure of RDV within the capsid remains unknown. We present here the 3D structures of RDV particles that are composed of different components, as determined by cryo-electron microscopy (cryo-EM) and 3D reconstruction, which we determined in order to investigate the internal structure of RDV and which provide clues to the organization of proteins and dsRNA in intact RDV.

Materials and Methods

Preparation of fRDV, eRDV and VLP for cryo-EM

The O strain of RDV (*13*) was purified as described by Omura *et al.* (*14*). Intact particles (fRDV) and empty particles (eRDV) were separated by sucrose density-gradient centrifugation and their components were analysed by electrophoresis. Virus-like particles (VLP) composed of P3 and P8 proteins, were purified as described previously (*15*). Component proteins of VLP were analysed by SDS–PAGE and western blotting with RDV P3- and P8-specific antibodies (*3*).

Cryo-EM and imaging procedures

Samples of RDV, including fRDV and eRDV, were embedded in vitreous ice and examined by cryo-EM at a nominal magnification of 28,000 × and an operating voltage of 120 kV. Each area of a specimen was recorded twice at focal pairs with defocus values of 1.0 and 3.0 μm, respectively. The fRDV and the eRDV were distinguishable in the far-defocus images, and were boxed separately. The initial origins and orientations of selected particle images were obtained by polar Fourier transform procedures (*16*, *17*), with the previous run of the density map used as the initial model (*18*). This procedure was followed by inter-particle orientation refinement with cross-common lines procedures. The VLPs were examined with an electron microscope JEM-2100 (JEOL, Japan) operated at 200 kV with a nominal magnification of 30,000×, and images were recorded with a 4k × 4k charge-coupled device (CCD). The final reconstructions of fRDV, eRDV and VLP were computed from 689, 146 and 467 particles at 26, 32 and 27 Å resolution, respectively. The resolution was assessed using the 0.5 threshold in the Fourier shell correlation between two reconstructions calculated from halves of the data set. For further analysis at higher resolution, samples of fRDV were embedded in vitreous ice and examined at temperatures between 4 K and 20 K with an electron microscope (JEM-3000SFF; JEOL, Japan) equipped with a liquid-helium stage and operated at 300 kV. Electron micrographs were recorded on Kodak SO-163 film (Eastman Kodak Co., NY) at a magnification of 40,000×, and were digitized with a microdensitometer (Carl Zeiss, Germany) with sampling at 1.25 Å/pixel. The scanned images were boxed, and the origins and orientations of particles were estimated and refined as described above. The final reconstruction of fRDV was further computed by averaging 3399 images at a resolution of 20 Å.

Calculation of the concentration of RNA and visualization of the RNA density

The volumes of interior space of BTV, reovirus and RDV were calculated based on the atomic structures of the capsid shells (*4*, *7*, *9*). The concentration of RNA was calculated after subtracting the volume of the transcriptional enzymes from the volume of the interior spaces. To show RNA density, it was cut away from the full RDV reconstruction with a mask that covered the interior space of the capsid shell, and it was visualized in program O (*19*). In addition, the RNA density was cut away between radii of 230 and 260 Å to show the first layer of RNA and between radii of 200 and 230 Å to show the second layer of RNA. B-form RNA duplexes were fitted manually into the rod-shape densities in the first and the second layers of RNA.

Results

Comparison of overall structures

Analysis by SDS–PAGE indicated that both the fRDV and eRDV particles contained all the internal component proteins, including the P1, P5 and P7 proteins (Fig. 1B). However, eRDV particles lacked all 12 segments of dsRNA (data not shown). In cryo-EM micrographs, the fRDV particles were easily distinguishable from the eRDV particles by the presence, in fRDV, of RNA density in the centre of each particle (Fig. 1A). The structures of the double-layered capsid shells were almost identical, in terms of size and appearance, in fRDV, eRDV and the VLP (Fig. 1C–E). Furthermore, the atomic structure of the capsid (*4*) fitted the cryo-EM map well and without adjustments. The interior surface of the capsid shell of the VLP was smooth, while that of the eRDV had a globular density at each icosahedral 5-fold axis. The fRDV particle had at least three concentric spherical layers of density closest to the capsid shell, with the layers closer to the capsid being more ordered than those farther away (Fig. 2A and B). These structural observations, together with the results of biochemical analysis, indicated that the globular density at each icosahedral 5-fold axis and the concentric layers of density are represented transcriptional enzymes and the dsRNAs of the virus, respectively.

Organization of dsRNA in several concentric layers

As seen in the cross-section of the fRDV map, RNA was organized in concentric layers beneath the capsid shell. In the outermost layer of RNA, we observed parallel three-rod-shaped densities (Fig. 3A), similar to those that had been generated previously in structural analysis of reoviruses that involved cryo-EM reconstruction (*8*, *10*). We assumed that these density features corresponded to ordered dsRNA, and we attempted to fit atomic models of dsRNA duplexes into the rod-shaped densities. The atomic models were easily accommodated by the rod-shaped density segments. The length of nucleotides that fitted into the outermost layer of RNA in the asymmetric unit of the icosahedral symmetry was equivalent to 90 bp. In the second layer of RNA, two rod-shaped densities ran parallel to each other, and dsRNA duplexes composed of 30 bp were fitted into these rod-shaped densities, with the diameter of each bundle of density being consistent with the diameter of a dsRNA duplex, namely 20 Å. These segments were found parallel to the rod-shaped densities in the outermost layer of RNA (Figs. 3B and D), which were arranged in a columnar hexagonal phase, with the distances between RNA duplexes being 32–35 Å approximately (Figs. 3D and E). The ordered RNA in the first and second layers accounted for about 7,200 bp (7.2 kb) out of a total of 25.7 kb in the genome, namely, 28% of the total genome.

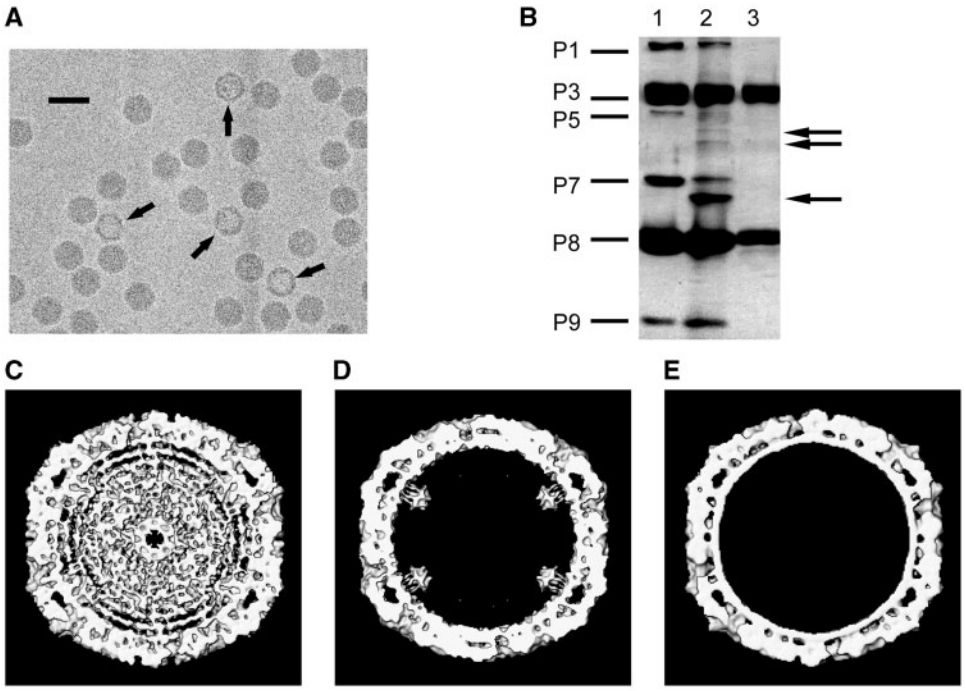

Fig. 1 Comparison of the structures of fRDV, eRDV and VLP. (A) Electron micrograph of ice-embedded RDV particles. The arrows indicate eRDV. The bar represents 100 nm. (B) Sodium dodecyl sulphate–10% polyacrylamide gel electrophoresis of proteins from the fRDV (lane 1), eRDV (lane 2) and VLP (lane 3). Positions of RDV protein species are shown. The bands between P7 and P8 proteins and between P5 and P7 proteins in the eRDV particle (indicated by arrows) are the contaminant host protein, which locates at the same position in the sucrose gradient centrifugation during purification (*29*). (C–E) Central cross-sections (40 Å thick) from the maps of the fRDV (C), eRDV (D) and VLP (E).

Concentration of dsRNA inside the capsid

The genome of RDV is encapsidated by the capsid shell, and its replication occurs within the intact capsid shell. We calculated the concentration of dsRNA within the capsid shell and compared it with that in other reoviruses. The interior volume was defined by the atomic model of the capsid shell, as determined by X-ray crystallography, and estimated to be 73.0×10^6 Å^3. Since the volume of the 12 TCs of RDV was estimated to be 7.8×10^6 Å^3, from an average partial volume of 0.74 cm^3/g (1.23 Å^3/Da) for proteins (*20*), we estimated that the space remaining for the genome of RDV was 65.2×10^6 Å^3. Under these conditions the concentration of dsRNA within the capsid shell was estimated to be 420 mg/ml (Table I).

The ordered volume of the transcription complex at the 5-fold axis

Comparisons between fRDV and eRDV revealed the molecular boundary between the TC and the dsRNA in the fRDV particle (Fig. 1C and D). From this comparison, we estimated that the mass volume of a TC in the fRDV particle was 3.5×10^5 Å^3 (Figs 2C and D). Since the estimated volumes of a TC and five molecules of P7 were 6.5×10^5 Å^3 (for 530 kDa; one copy each of P1 and P5, and five copies of P7) and 3.4×10^5 Å^3 (for 275 kDa; five copies of P7), respectively, the ordered volume (3.5×10^5 Å^3) corresponded to 54% occupancy of the estimated volume of a TC and was consistent with the estimated volume of five P7 molecules (100% occupancy) if all of the ordered volume is attributable to P7 molecules. Thus, the well-ordered densities were attributed to five molecules of P7 (Figs 2C and D). The density of a P7 molecule could be divided into two domains, the top and the bottom domain (Fig. 2D). The top domain was located just beneath the P3 capsid shell, binding to P3 and dsRNA. The bottom domain was located closer to the inside of the viral particle and was twisted in a left-handed manner relative to the top domain.

Discussion

The RDV capsid forms a spherical compartment, which provides a site for the replication of the viral genome, by encapsidating 12 segments of dsRNA and the enzymes required for transcription. Comparisons of particles composed of different components allowed us to determine the functional organization of the internal components. Comparisons between eRDV and VLP revealed the globular density at each icosahedral 5-fold axis (Fig. 1D and E), which was considered to be the transcription complex (TC), given the facts that (i) the ordered density attached to the P3 inner capsid protein was that of P7, when fRDV was observed by X-ray crystallography (*4*); (ii) the P7 protein has the ability to bind dsRNA (*21*, *22*) and also the P1 protein (*21*); and (iii) that the P1, P5 and P7 proteins bind viral transcripts (*22*). The globular density was connected to the density of the P3 inner capsid layer at two sites (major- and minor-binding sites; Figs. 2C and D), one of which coincided with the ordered density of P7, as visualized

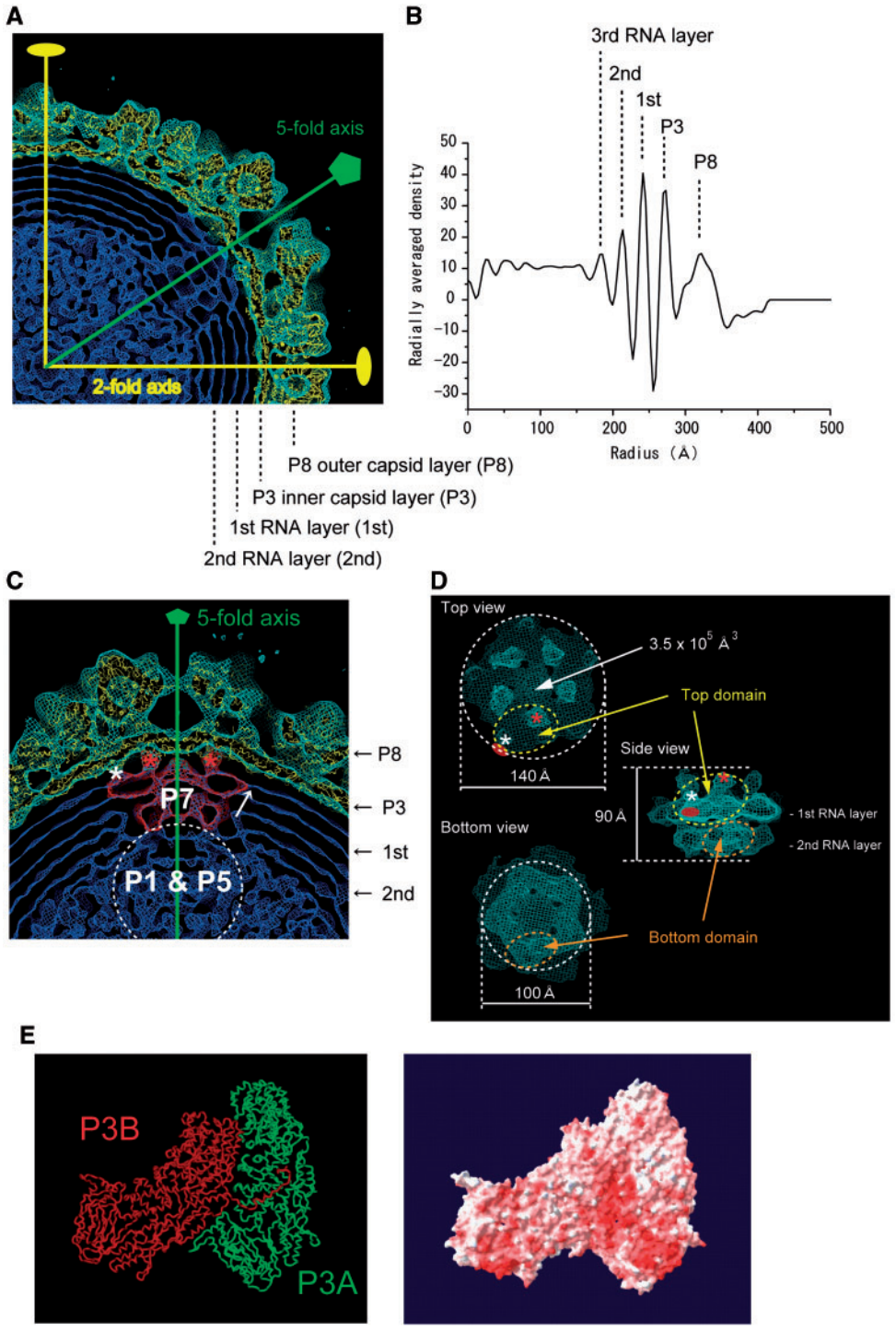

Fig. 2 Cryo-EM density map of fRDV at 20 Å resolution, showing RNA densities. (A) Central cross-section from the map of fRDV. The capsid and RNA regions are coloured cyan and blue, respectively. Atomic models of P3, P8 and P7 proteins are fitted into the fRDV cryo-EM map. Atomic models are shown in yellow. (B) Radial density distribution of reconstructed fRDV. The radial positions of structural components are indicated. (C) A small portion of the region whereby P7 binds to the P3 capsid shell. Binding of P7 protein to the P3 capsid shell is indicated by asterisks (red, major-binding site; white, minor-binding site). The red asterisks show binding sites revealed by X-ray crystallography. The connection of density between the P7 protein and the RNA layer is indicated by a white arrow. (D) Top view: cryo-EM map of pentameric P7 proteins in fRDV viewed from the outside of the particle. Sites of binding to the P3 capsid shell are indicated by asterisks (red, major-binding site; white, minor binding site). The red asterisk is the binding site revealed by X-ray crystallography. The red ellipse indicates the site of binding of P7 to RNA. The volume mass is indicated. Side view: Cryo-EM map after rotation of the top view by 90°. Bottom view: Cryo-EM map viewed from the inside of the particle. (E) Cα-trace of the P3A and P3B asymmetric dimer (*4*, *30*) and the surface electrostatic potentials on the dimer, as viewed from the inside of the viral particle. P3A and P3B subunits in the Cα-trace are coloured green and red, respectively. In the right panel, positively charged regions are coloured blue and negatively charged regions are coloured red.

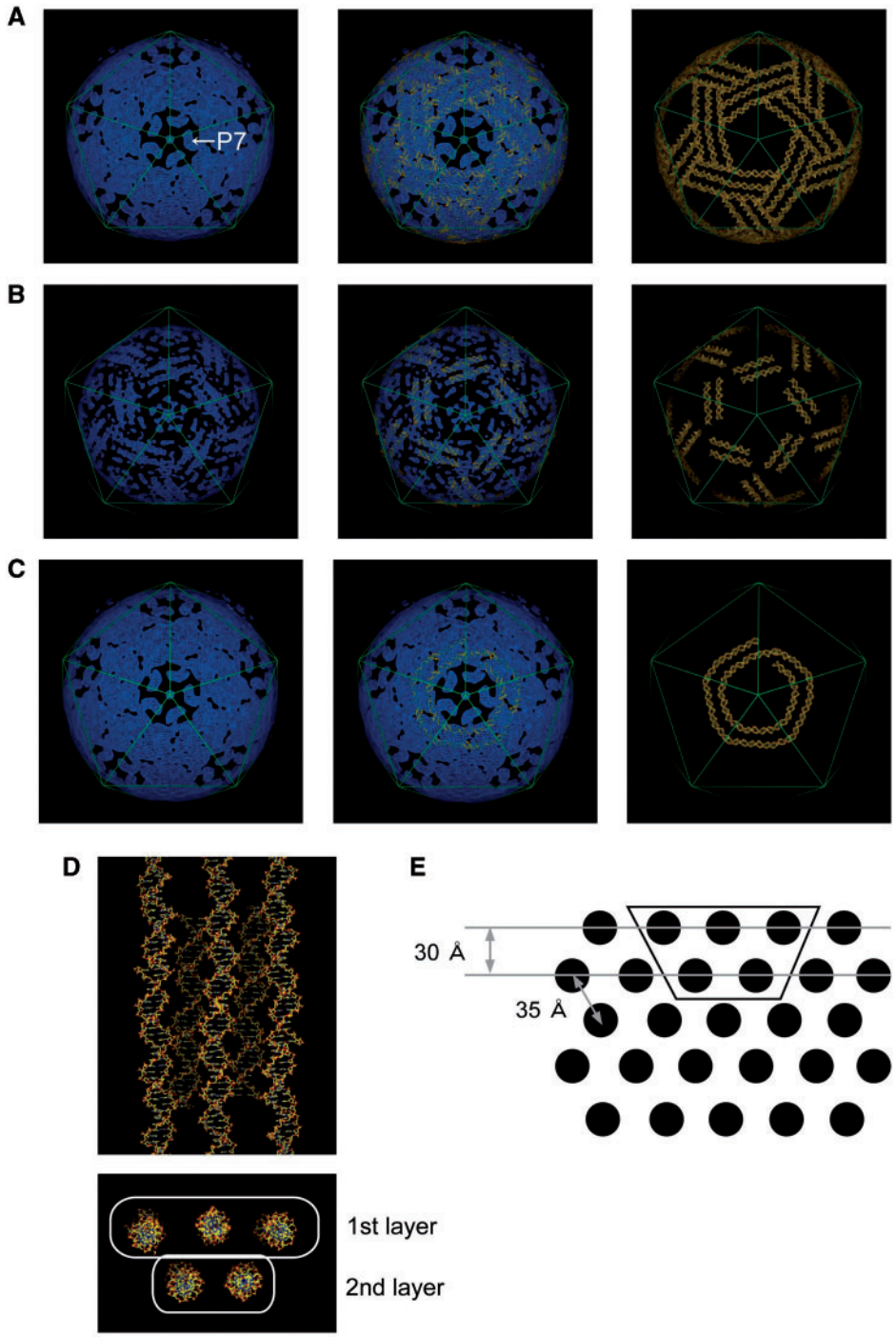

Fig. 3 Fitting of dsRNA models into rod-shaped densities in the RNA layer. (A) Left, cryo-EM map of the first layer of RNA; middle, cryo-EM map of the first layer of RNA with fitted B-form RNA duplexes; right, fitted B-form RNA duplexes. (B) Left, cryo-EM map of the second layer of RNA; middle, cryo-EM map of the second layer of RNA with fitted B-form RNA duplexes; right, fitted B-form RNA duplexes. (C) Models of the spiral organization of dsRNA in an RDV particle. One segment of dsRNA binds to five molecules of P7 protein around the 5-fold axis, and these interactions between P7 proteins and dsRNA generate the spiral organization of dsRNA in the viral capsid shell. (D) Packing of the dsRNA duplexes within the RDV capsid shell, as viewed from the outside of an RDV particle (upper panel), and the appearance after rotation of the upper image by 90° (lower panel). (E) Schematic representation of the arrangement of nucleic acids in the columnar hexagonal phase.

by X-ray crystallography. The density was divided into five regions around the icosahedral 5-fold axis (Fig. 2D), in agreements with the observation, by X-ray crystallographic analysis, that a small polypeptide region of P7 was evident at five regions on the 5-fold axes of RDV. Thus, we attributed the outermost region of the globular density to five P7 molecules, and we suggest that the TC is anchored to the viral capsid via the P3–P7 interactions. The reason why only a small polypeptide region of P7 is evident by X-ray crystallography at 3.5 Å resolution is considered that the other region of the P7 is not ordered at such

Table I. Internal volumes and RNA densities inside the capsid shells of three reoviruses.

	RDV	BTV	Reovirus
Internal volume (Å^3)	73.3×10^6	57.3 (60.6[a]) $\times 10^6$	60.9×10^6
Volume of RNA region (Å^3)	63.6×10^6	47.8 (53.0[a]) $\times 10^6$	55.5×10^6
Density of RNA (mg/ml)	430	450 (410[a])	450
Viral genome	25.7 kb/16.4 MDa/12 seg.	19.2 kb/13.1 MDa/10 seg.	23.5 kb/15 MDa/10 seg.
Protein components (Name/md.wt.copy number per virion)	P1/164K/12 P5/91K/12 P7/55K/60	VP1/150K/12 VP4/76K/24 VP6/36K/72	λ3/142K/12 μ2/83K/24
Total mol.wt. of internal proteins per virion	6360 kDa	6216 kDa	3696 kDa
Volume of TC (Å^3)	9.4×10^6	9.2 (7.6[a]) $\times 10^6$	5.5×10^6

[a]Values reported previously by Gouet *et al.* (*23*).

high resolution (*4*). Indeed, a globular density for the transcription complex including the P7 protein was visible at each 5-fold vertex at lower resolution (*31*). By the same reason, the globular density was visible at lower resolution by cryo-EM, analysed here. Although there is no evidence for the P1 and P5 protein localization, we assumed that they locate underneath the P7 pentamer (Fig. 2C) based on the facts that the P1 and P5 proteins bind to the P7 protein and are supposed to form the TC at each 5-fold vertex, while the P7 proteins are surrounded by dsRNA and their sides are occupied by them as described below.

Locating the TC at the 5-fold axes appears a common feature in reoviruses: rotavirus (*8*), BTV (*23*, *24*) and CPV (*10*). This might be related to efficient translocation of nascent mRNA through the junction of the five subunits around the vertices of the capsid shell. Actually, in the case of the rotavirus the extruding mRNAs through the 5-fold axes are visualized by cryo-EM reconstruction (*25*, *26*). Comparison of fRDV and eRDV by both cryo-EM and analysis by SDS–PAGE of their nucleic acids (data not shown) demonstrated that the components of the circular concentric layers were the dsRNAs of RDV. The outermost layer of RNA was connected to five density fragments of P7 (Figs. 3A, 2C and D) and the connections of densities imply interactions between the dsRNA and the P7 protein around the 5-fold axis of the particle. Such organization result in better ordered RNA density in the region close to the interior capsid surface than that far from reaching the capsid shell.

The dsRNA was organized as concentric layers. In the first outermost and the second layer of RNA, in particular, we observed parallel strands of rod-shaped densities. In RDV, the rod-shaped densities were not perpendicular to the icosahedral edge that connects the adjacent icosahedral 5-fold axes (Fig. 3). Since one rod-shaped density in the outermost layer of RNA is attached to the density of P7 protein, as described above; the direction of the parallel strands would be determined by the distribution of the polypeptide regions that are responsible for binding of RNA to the five molecules of P7 protein (*2*). Since the P7 protein has non-specific nucleic acid-binding activity (*21*, *22*), one segment of dsRNA might bind to several molecules of P7 and, probably, binds to five P7 molecules at the 5-fold axes, in a sequence-non-specific manner. Thus, each set of pentameric P7 complexes at the icosahedral vertex might be surrounded by one segment of a dsRNA molecule (Fig. 3C). The following dsRNA region goes parallel to the P7 bound dsRNA, and surrounds further the P7 pentamer (Fig. 3C). When the dsRNA duplex encounters with other dsRNA duplex from the neighbouring vertex, it moves to the second RNA layer, where it also goes parallel to the dsRNA duplex in the first RNA layer. Thus, the dsRNA around the 5-fold axis adopts a spiral organization at liquid crystalline state (Fig. 3C and D). The liquid crystalline array is a stable state in the RNA concentration inside the capsid shell as described below. As a result, it is likely that one segment of dsRNA is threaded into one transcriptional complex at each icosahedral vertex in each particle of RDV. In such a structure, individual TCs could function independently to replicate the 12 corresponding segments of the genome simultaneously.

Within the capsid shell, dsRNA duplexes formed liquid crystalline arrays (Figs. 3D and E) in the columnar hexagonal phase, as reported previously (*27*). The layers of RNA in RDV are separated by 30 Å. When compared with the 27 Å spacing in CPV (*10*), the 30 Å spacing in BTV (*23*) and the 31 Å spacing in rotavirus (*28*), the spacing of RDV dsRNA suggests that it is packed similarly to the dsRNA in the members of Reoviridae family analysed to date. Such common spacing might be due to the repulsion of negatively charged neighbouring columns of dsRNA, facilitating the smooth movement of the dsRNA during transcription. In this context, the electrostatic status of the inner surface of the P3 capsid shell was considered to be negatively charged (data not shown) and would repel negatively charged dsRNA. Indeed, as expected, it was negatively charged (Fig. 2E), and no significant connection between the P3 capsid shell and the RNA layer was observed (Fig. 2A and C). In contrast, there were positively and negatively charged clusters at the lateral faces between P8 trimers, which are required for lateral binding. The negatively charged clusters in the P3 core capsid protein and the positively charged clusters in the P8 outer capsid proteins are required for the vertical binding of the core and outer capsid proteins of RDV (*4*). The interior concentrations of nucleic acid within the capsids of BTV and reovirus are similar to that of RDV (Table I), even though the lengths of the genome and the numbers of dsRNA segments differ

significantly among them (*9*, *23*). The packaging of nucleic acid in the liquid crystalline state might be optimized to prevent the entanglements among the RNA segments. Thus the spiral organization of the liquid crystalline dsRNA, guided by the positioning of P7, allows the dsRNA to be processed efficiently when RDV extrudes nascent mRNA into infected cells.

Funding

The authors are grateful for the financial support provided by USDA, NIH Roadmap and the STINT Foundation (to R.H.C.). Part of this study was supported by the 21st Century Centers of Excellence (COE) Program and by a Grant-in-Aid for Scientific Research on Priority Area ('Structures of Biological Macromolecular Assemblies'), from the Ministry of Education, Culture, Sports, Science and Technology of Japan, and by the Program for Promotion of Basic Research Activities for Innovative Biosciences (PROBRAIN to T.O.).

Conflict of interest

None declared.

References

1. Omura, T., and Yan, J. (1999) Role of outer capsid proteins in transmission of *Phytoreovirus* by insect vectors. *Adv. Virus Res.* **54**, 15–43
2. Zhong, B.X., Shen, Y.W., and Omura, T. (2005) RNA-binding domain of the key structural protein P7 for the *Rice dwarf virus* particle assembly. *Acta Biochim. Biophys. Sin* **37**, 55–60
3. Miyazaki, N., Hagiwara, K., Naitow, H., Higashi, T., Cheng, R.H., Tsukihara, T., Nakagawa, A., and Omura, T. (2005) Transcapsidation and the conserved interactions of two major structural proteins of a pair of phytoreoviruses confirm the mechanism of assembly of the outer capsid layer. *J. Mol. Biol.* **345**, 229–237
4. Nakagawa, A., Miyazaki, N., Taka, J., Naitow, H., Ogawa, A., Fujimoto, Z., Mizuno, H., Higashi, T., Watanabe, Y., Omura, T., Cheng, R.H., and Tsukihara, T. (2003) The atomic structure of *Rice dwarf virus* reveals the self-assembly mechanism of component proteins. *Structure* **11**, 1227–1238
5. Zhong, B., Kikuchi, A., Moriyasu, Y., Higashi, T., Hagiwara, K., and Omura, T. (2003) A minor outer capsid protein, P9, of *Rice dwarf virus*. *Arch. Virol.* **148**, 2275–2280
6. Hill, C.L., Booth, T.F., Prasad, B.V., Grimes, J.M., Mertens, P.P., Sutton, G.C., and Stuart, D.I. (1999) The structure of a cypovirus and the functional organization of dsRNA viruses. *Nat. Struct. Biol.* **6**, 565–568
7. Grimes, J.M., Burroughs, J.N., Gouet, P., Diprose, M., Malby, R., Zientara, S., Mertens, P.P., and Stuart, D.I. (1998) The atomic structure of the bluetongue virus core. *Nature* **395**, 470–478
8. Prasad, B.V.V., Rothnagel, R., Zeng, C.Q.-Y., Jakana, J., Lawton, J.A., Chiu, W., and Estes, M.K. (1996) Visualization of ordered genomic RNA and localization of transcriptional complexes in rotavirus. *Nature* **382**, 471–473
9. Reinisch, K.M., Nibert, M.N., and Harrison, S.C. (2000) Structure of the reovirus core at 3.6 Å resolution. *Nature* **404**, 960–967
10. Xia, Q., Jakana, J., Zhang, J.Q., and Zhou, Z.H. (2003) Structural comparisons of empty and full cytoplasmic polyhedrosis virus. Protein-RNA interactions and implications for endogenous RNA transcription mechanism. *J. Biol. Chem.* **278**, 1094–1100
11. Miyazaki, N., Uehara-Ichiki, T., Xing, L., Bergman, L., Higashiura, A., Nakagawa, A., Omura, T., and Cheng, R.H. (2008) Structural evolution of reoviridae revealed by oryzavirus in acquiring the second capsid shell. *J. Virol.* **82**, 11344–11353
12. Zhang, X., Walker, S.B., Chipman, P.R., Nibert, M.L., and Baker, T.S. (2003) Reovirus polymerase λ3 localized by cryo-electron microscopy of virions at a resolution of 7.6 Å. *Nat. Struct. Biol.* **10**, 1011–1018
13. Kimura, I., Minobe, Y., and Omura, T. (1987) Changes in a nucleic acid and a protein component of *Rice dwarf virus* particle associated with an increase in symptom severity. *J. Gen. Virol.* **68**, 3211–3215
14. Omura, T., Yan, J., Zhong, B., Wada, M., Zhu, Y., Tomaru, M., Maruyama, W., Kikuchi, A., Watanabe, Y., Kimura, I., and Hibino, H. (1998) The P2 protein of Rice dwarf phytoreovirus is required for adsorption of the virus to cells of the insect vector. *J. Virol.* **72**, 9370–9373
15. Hagiwara, K., Higashi, T., Namba, K., Uehara-Ichiki, T., and Omura, T. (2003) Assembly of single-shelled cores and double-shelled virus-like particles after baculovirus expression of major structural proteins P3, P7 and P8 of *Rice dwarf virus*. *J. Gen. Virol.* **84**, 981–984
16. Cheng, R.H., Reddy, V.S., Olson, N.H., Fisher, A.J., Baker, T.S., and Johnson, J.E. (1994) Functional implications of quasi-equivalence in a *T*=3 icosahedral animal virus established by cryo-electron microscopy and X-ray crystallography. *Structure* **2**, 271–282
17. Baker, T.S., and Cheng, R.H. (1996) A model-based approach for determining orientations of biological macromolecules imaged by cryoelectron microscopy. *J. Struct. Biol.* **116**, 120–130
18. Wu, B., Hammar, L., Xing, L., Markarian, S., Yan, J., Iwasaki, K., Fujiyoshi, Y., Omura, T., and Cheng, R.H. (2000) Phytoreovirus T=1 core plays critical roles in organizing the outer capsid of T=13 quasi-equivalence. *Virology* **271**, 18–25
19. Jones, T.A., Zou, J.-Y., Cowan, S.W., and Kjeldgaard, M. (1991) Improved methods for building protein models in electron density maps and the location of errors in these models. *Acta Crystallogr. A* **47**, 110–119
20. Kantardjieff, K.A., and Rupp, B. (2003) Matthews coefficient probabilities: iImproved estimates for unit cell contents of proteins, DNA, and protein-nucleic acid complex crystals. *Protein Sci.* **12**, 1865–1871
21. Ueda, S., Masuta, C., and Uyeda, I. (1997) Hypothesis on particle structure and assembly of rice dwarf phytoreovirus: interactions among multiple structural proteins. *J. Gen. Virol.* **78**, 3135–3140
22. Zhong, B., Roth, D.A., Zhu, Y., and Omura, T. (2004) An assembly model of *Rice dwarf virus* particle. *Science China Ser. Life Sci.* **47**, 92–100
23. Gouet, P., Diprose, J.M., Grimes, J.M., Malby, R., Burroughs, J.N., Zientara, S., Stuart, D.I., and Mertens, P.P.C. (1999) The highly ordered double-stranded RNA genome of bluetongue virus revealed by crystallography. *Cell* **97**, 481–490
24. Nason, E.L., Rothagel, R., Mukherjee, S.K., Kar, A.K., Forzan, M., Prasad, B.V., and Roy, P. (2004) Interactions between the inner and outer capsids of bluetongue virus. *J. Virol.* **78**, 8059–8067
25. Lowton, J.A., Estes, M.K., and Prasad, B.V. (1997) Three-dimensional visualization of mRNA release from actively transcribing rotavirus particles. *Nat. Struct. Biol.* **4**, 118–121
26. Lowton, J.A., Estes, M.K., and Prasad, B.V. (2000) Mechanism of genome transcription in segmented dsRNA viruses. *Adv. Virus Res.* **55**, 185–229

27. Livolant, F., and Leforestier, A. (1996) Condensed phases of DNA: structures and phase transitions. *Prog. Polym. Sci.* **21**, 1115–1164
28. Pesavento, J.B., Lawton, J.A., Estes, M.K., and Prasad, B.V.V. (2001) The reversible condensation and expansion of the rotavirus genome. *Proc. Natl Acad. Sci. USA* **98**, 1381–1386
29. Zhong, B., Roth, D.A., Zhu, Y., and Omura, T. (2004) An assembly model of *Rice dwarf virus* particle. *Sci. China Ser. C* **47**, 92–100
30. Hagiwara, K., Higashi, T., Miyazaki, N., Naitow, H., Cheng, R.H., Nakagawa, A., Mizuno, H., Tsukihara, T., and Omura, T. (2004) The amino-terminal region of major capsid protein P3 is essential for self-assembly of single-shelled core-like particles of *Rice dwarf virus*. *J. Virol.* **78**, 3145–3148
31. Naitow, H., Morimoto, Y., Mizuno, H., Kano, H., Omura, T., Koizumi, M., and Tsukihara, T. (1999) A low-resolution structure of *rice dwarf virus* determined by *ab initio* phasing. Acta Crystallogr. *D* **55**, 77–84